the intensity of heat exchange between the phases; C_d, the coefficient of particle aerodynamic drag; Nu, Nusselt number; Re_{12}, Reynolds number for the streamlining of the particles; Pr, Prandtl number; d, the particle diameter; R, the radius of the apparatus. Subscripts: i = 1, gas; i = 2, particles; k, the summation index; ∞, the parameters have been taken at the section AB; w, indicates that the parameters have been taken at the section ME; r, φ, z, the axes of the cylindrical coordinate system.

LITERATURE CITED

1. V. D. Goryachev, V. V. Chernyshev, and R. P. Kornev, Izv. Vyssh. Uchebn. Zaved., Énergetika, No. 3, 67-72 (1984).
2. B. S. Sazhin, B. P. Lukachevskii, M. Sh. Dzhunisbekov, et al., Teor. Osnovy Khim. Tekhnol., 19, No. 5, 687-690 (1985).
3. R. I. Nigmatullin, The Fundamentals of the Mechanics of Heterogeneous Media [in Russian], Moscow (1978).
4. O. M. Belotserkovskii and Yu. M. Davydov, The Method of Large-Scale Particles in Gasdynamics. Experimental Calculations [in Russian], Moscow (1982).
5. É. F. Shurgal'skii, Inzh.-Fiz. Zh., 49, No. 1, 51-57 (1985).

ISOTHERMAL AXISYMMETRIC FLOW OF AN INCOMPRESSIBLE FLUID IN RADIAL CONTACT APPARATUS

P. G. Shtern, E. A. Rudenchik, S. V. Turuntaev,
I. S. Luk'yanenko, E. G. Bezrukova, and E. K. Popov

UDC 552.546

A method is proposed for the calculation of the axisymmetric flow of an incompressible fluid in a radial apparatus with a nonmoving layer of granular material. An engineering method is developed to evaluate the degree of flow nonuniformity in equipment of this type, thus making it possible operationally to choose among structural solutions in the design of this equipment.

A number of research studies [1-4] have been devoted to the theoretical and experimental study of flow distributions in perforated channels and radial reactors. The energy approach within the framework of a one-dimensional model is utilized in calculating the distributions of flows in perforated channels [1, 2]. The flow model for radial equipment with a nonmoving granular layer, such as that proposed in [3], is valid for low velocities when the resistance to the flow within the catalyst layer depends linearly on the rate of filtration. There is no doubt as to the importance of calculating the flow in industrial reactors, where the quadratic relationship between the pressure drop across the layer and velocity is valid.

Let us examine the axisymmetric flow of an incompressible fluid in an apparatus whose diagram is shown in Fig. 1a. The granular layer is situated between two coaxial perforated cylinders. The fluid flows into the apparatus at a velocity v_{in} through a distributing collector I, passes through to the operating zone III, and is discharged from the apparatus through the outside collector II at a velocity v_{out}. The following circuits may be regarded as special cases: a perforated channel with a dead end (zone I); an apparatus in which the atmosphere functions as zone II (zones I and III).

The mathematical model is based on the assumption that the fluid is incompressible:

$$\operatorname{div} \mathbf{v} = 0, \tag{1}$$

Synthetic Rubber Monomer Scientific-Research Institute, Yaroslavl'. Translated from Inzhenerno-Fizicheskii Zhurnal, Vol. 56, No. 4, pp. 555-562, April, 1989. Original article submitted September 16, 1987.

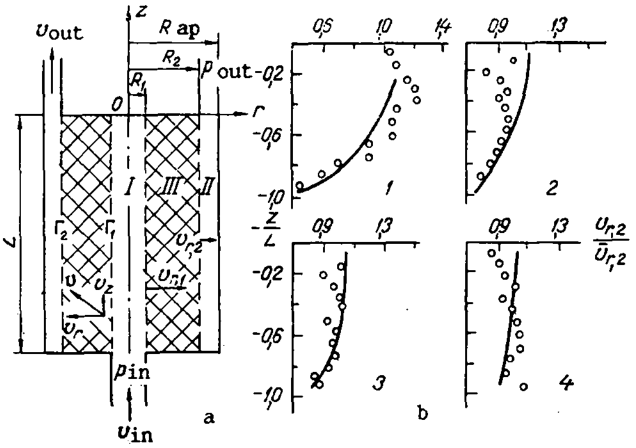

Fig. 1. Diagram of contact apparatus with radial liquid or gas inlet (a); theoretical (solid lines) and experimental (points) relationships between the relative values of the radial velocity component at the outlet from the granular layer (boundary Γ_2) and the height of the apparatus (L = 0.8 m, R_1 = 0.065 m, R_2 = 0.185 m, $R_{ap} = \infty$) [4] (b): 1) f = 8580 kg/m^4; 2) 13,330; 3) 16,800; 4) 25,500.

in regions I and II we have the potential flow

$$\mathrm{rot}\,\mathbf{v} = 0, \tag{2}$$

while in the granular layer (zone III) the Ergun quadratic law is valid [5]:

$$\nabla p = -f\,|\mathbf{v}|\,\mathbf{v}. \tag{3}$$

The pressure within the collectors is determined from the Bernoulli law:

$$p = \frac{1}{2}\rho\,|\mathbf{v}|^2 = \mathrm{const}. \tag{4}$$

The boundary conditions make provision for the continuity of the pressure field and of the normal velocity components at the boundaries of the layer, which follows from the equations for the conservation of mass and momentum.

The existence of perforations at the boundaries of zones Γ_1 and Γ_2 leads to a situation in which the pressure undergoes a jump on transition from one zone to another, and the magnitude of this discontinuity is determined from the law governing the drag generated by the perforations [6]:

$$\Delta p_{1,2} = \sigma_{1,2}\,(v_{r,1,2})^2. \tag{5}$$

It was suggested in [2] to use the following formula to calculate the perforation drag, which corresponds to the average rate of flow through the boundary between the zones:

$$\sigma = \frac{\rho}{2}\left[\varphi^{-1}\left(1 - \varphi + \sqrt{\frac{1-\varphi}{2}}\right)\right]^2.$$

Let us write the continuity equation (1) in terms of the stream function Ψ: $v_r = (1/r)/(\partial\Psi/\partial z)$, $v_z = -(1/r)(\partial\Psi/\partial r)$. The potentiality condition (2) indicates that the stream function in regions I and II satisfies the Laplace equation

$$\left(\frac{\partial_2}{\partial r^2} + \frac{\partial^2}{\partial z^2}\right)\Psi = 0. \tag{6}$$

The equality of the pressure derivatives combined with the Ergun law yields the following nonlinear elliptical equation for zone III:

$$(|\mathbf{v}|^2 + v_r^2)\frac{\partial^2\Psi}{\partial z^2} + (|\mathbf{v}|^2 + v_z^2)\frac{\partial^2\Psi}{\partial r^2} - 2v_r v_z\frac{\partial^2\Psi}{\partial z\partial r} + 2v_z|\mathbf{v}|^2 + r|\mathbf{v}|^2\left(v_r\frac{\partial \ln f}{\partial z} - v_z\frac{\partial \ln f}{\partial r}\right) = 0. \tag{7}$$

Our attention is drawn to the fact that if the normal component of the velocity at the boundary of the zone is given, i.e., the values of the stream functions at the boundaries have been determined, only a single solution exists for the elliptical equation.

The solution of Eqs. (6) and (7) and the calculation of the pressures in each zone of the reactor for given normal velocity components at the boundaries of zones Γ_1 and Γ_2 will be referred to as the solution of the direct problem. However, generally speaking, this solution does not provide for satisfaction of the boundary conditions with respect to pressure. In order to find that single solution which satisfies all of the boundary conditions we have to solve the inverse problem, and namely, to find the normal velocity components at the boundaries of Γ_1 and Γ_2 such that conditions (5) will be satisfied at these boundaries. Mathematically, this problem can be formulated as the problem of seeking out the minimum functional

$$\Phi(v_{r,1};\ v_{r,2}) = \frac{1}{L}\int_{\Gamma_1} (p_1^{\mathrm{I}} - p_1^{\mathrm{III}} - \Delta p_1)^2 dz + \frac{1}{L}\int_{\Gamma_2} (p_2^{\mathrm{II}} - p_2^{\mathrm{III}} - \Delta p_2)^2 dz, \tag{8}$$

where the pressure in zones I and II at boundaries Γ_1 and Γ_2 are determined from the Bernoulli equation (4):

$$p_1^{\mathrm{I}} = p_{\mathrm{in}} - \frac{\rho}{2}[v_{r,1}^2 + v_{z,1}^2],$$

$$p_2^{\mathrm{II}} = p_{\mathrm{out}} - \frac{\rho}{2}[v_{r,2}^2 + v_{z,2}^2],$$

while $\Delta p_{1,2}$ is determined from Eq. (5).

In order numerically to find the minimum of functional (8) it is necessary to give the function $v_{r1,2}$ a parametric representation by means of a finite number of independent parameters. Here it must be borne in mind that in view of the law of the conservation of mass $v_{r,1}$ and $v_{r,2}$ are related by the condition:

$$R_1\int_{\Gamma_1} v_{r,1}(z)\,dz = R_2\int_{\Gamma_2} v_{r,2}(z)\,dz.$$

In order to make it possible to select the parameters $v_{r,1}$ and $v_{r,2}$ independently, we will determine the velocity profiles of $\tilde{v}_{r,1}$ and $\tilde{v}_{r,2}$, normalized so that $R_1\int_{\Gamma_1}\tilde{v}_{r,1}(z)\,dz = R_2\int_{\Gamma_2}\tilde{v}_{r,2}(z)\,dz = 1$, and then we determine the amplitude of the velocity u: $v_{r,1} = u\tilde{v}_{r,1}$; $v_{r,2} = u\tilde{v}_{r,2}$. The numerical calculations demonstrated that for normalized profiles of $\tilde{v}_{r,1}$ and $\tilde{v}_{r,2}$ parametrization with three parabolas is quite satisfactory with a continuous first derivative at the joining points (quadratic splines). Each of these splines is defined by six parameters. We used the two coordinates of the joining points and four values of $\tilde{v}_{r,1}$ (or $\tilde{v}_{r,2}$) at fixed points as the parameters.

The relationship between functional (8) and the amplitude of the velocity is quadratic, and minimization of the functional on the basis of this parameter is accomplished analytically. Moreover, the minimization with respect to p_0 is also done analytically, i.e., the quantity which arises in the determination of pressure from the Ergun equation (3).

It is important to point out that in none of the numerical experiments, and hundreds of these were carried out for a variety of resistance factors and geometric dimensions of the apparatus, did we observe any local minima with values of $\Phi(v_{r,1};\ v_{r,2}) \neq 0$.

The feasibility of the theoretical model was verified on the basis of the experimental results for a channel with perforated walls [2] and for an apparatus in which the flow discharged into the atmosphere [4]. Figure 2 shows the theoretically derived values of the velocity v_z and the pressure in the distributing collector, as compared to the experimental values from [2]. We see that the results of the calculation are in good agreement with the measurement results and the curves obtained on the basis of the energy approach. Adequate agreement was shown by profiles for the radial velocity component at the outlet from the granular layer for the apparatus in which the flow was discharged into the atmosphere (see Fig. 1b), obtained theoretically and measured with a heat-sensing anemometer [4]. In addition, we might take

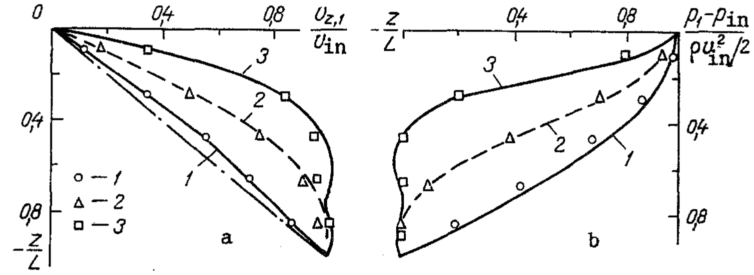

Fig. 2. Distributions of relative values for the axial velocity component (a) and the relative pressures (b) along the length of a perforated channel with a closed end: the solid lines indicate the numerical calculation performed by the authors; the dashed lines denote analytical calculations; the points indicate experimental data from [2]: 1) $\varphi = 0.04$; 2) 0.08; 3) 0.15.

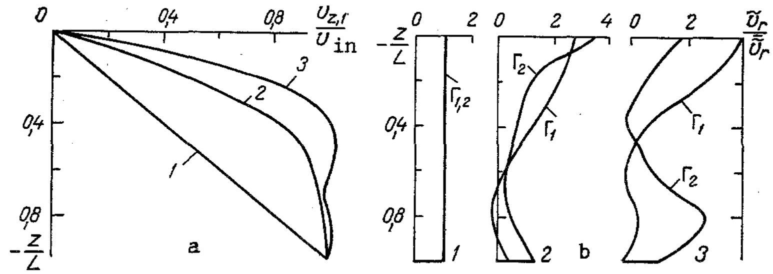

Fig. 3. The effect of layer resistance on the distributions of the relative values of the axial velocity component at the boundary Γ_1 (a) and the radial velocity component at the boundaries Γ_1 and Γ_2 (b) through the height of the apparatus, with the flow escaping to the atmosphere ($L = 1$ m, $R_1 = 0.053$ m, $R_2 = 0.3$ m, $R_{ap} = \infty$): f) $f = 52{,}000$ kg/m^4; 2) 1500 kg/m^4; 3) 65 mg/m^4.

note of the fact that as the resistance factor of the perforated channel increases (with a reduction in φ), we observe approximation of the distribution in the axial component of the velocity to the linear (Fig. 2), while with an increase in the resistance factor of the layer the profiles of the radial velocity components become increasingly uniform (see Fig. 1b).

The theoretical profiles of the axial and radial velocity components shown in Fig. 3 show that with an increase in resistance in the system the distribution of v_z in zone I tends to the linear, and the flow is uniformly distributed in the layer and the profile of v_r at the boundaries Γ_1 and Γ_2 within that layer becomes uniform. If the resistance of the system is not large, the nonuniformity of the flow increases sharply, and most markedly at the inlet into the layer.

Thus, the magnitude of the nonuniformity in a radial apparatus is characterized by deviation from the linear on the part of the distribution of the axial velocity component along the distributing collector.

These results make it possible to construct an engineering methodology for the evaluation of the degree of flow nonuniformity in a radial apparatus, such as may be necessary, for example, in the design of this equipment or to estimate the influence exerted by these nonuniformities on the processes occurring within the granular layer.

Let us consider an ideal reactor, i.e., a reactor with sufficiently great resistance, in which the pressure drop Δp_c across the distributing collector is considerably smaller than the total pressure difference Δp across the apparatus. In this case, as follows from the results of the numerical calculations (version 1 in Fig. 3), the axial velocity component $v_{z,1}$ at the boundary Γ_1 is linear with respect to z, while the radial velocity component $v_{r,1,2}$ is constant. Moreover, within the layer $v_z \ll v_r$, since $(\mathrm{grad}\,p)_r \gg (\mathrm{grad}\,p)_z$, and $f(r, z)$ is assumed to be constant.

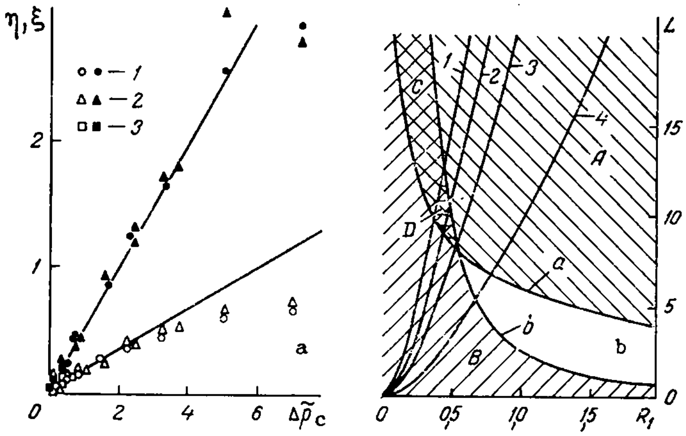

Fig. 4. Coefficients of flow-rate reduction (open circles) and degrees of flow nonuniformity (closed circles) as functions of the pressure difference across the distributing collector (a): 1) versions 1-11; 2) 12-19; 3) 20-23. Calculation of optimum dimensions of radial reactor (b): a) the function $L^2R_1 = Q^2f/4\pi^2\Delta p$; b) the function $LR_1{}^2 = \tau_I Q/\pi$; 1) $\xi = 0.2$; 2) 0.1; 3) 0.05; 4) 0.01. L, R_1, m.

TABLE 1. Calculated Versions of the Equipment and Their Parameters and Corresponding Values

Apparatus with flow outlet open to the atmosphere: L = 1m; R_1 = 0.053 m; R_2 = 0.3 m; R_{ap} = ∞, σ_2 = 0							Apparatus with outlet collect				
Unit No.	σ_1, kg/m³	f, kg/m⁴	Unit No.	σ_1, kg/m³	f, kg/m⁴	$\Delta\tilde{p}_c$	Unit No.	σ_1, kg/m³	σ_2, kg/m³	f, kg/m⁴	$\Delta\tilde{p}_c$
1	2300	51600	12	0	103200	0,20		$L=2,65$ m; $R_1=0,225$ m;			
2	1100	25250	13	0	50440	0,42					
3	575	13160	14	0	26320	0,80		$R_2=0,585$ m; $R_{ap}=0,7$ m;			
4	1100	0	»	»	»	0,83	20	900	2	5290	0,22
5	290	6580	15	0	13160	1,6	21	58	900	5290	0,39
6	65	7420	»	»	»	2,37	22	0	0	4230	0,61
7	190	4450	16	0	8900	2,37					
8	142	3290	17	0	6580	3,20		$L=7$ m; $R_1=0,6$ m;			
9	257	0	»	»	»	3,57					
10	90	2110	18	0	4210	5,00		$R_2=1,55$ m; $R_{ap}=1,85$ m;			
11	65	1480	19	0	2970	7,08	23	5	1235	10400	0,05

For such a reactor from Eq. (3) we have

$$\frac{\partial p}{\partial z} = -f|\mathbf{v}|v_z \approx 0; \quad \frac{\partial p}{\partial r} = -fv_r^2. \tag{9}$$

The continuity condition for the flow yields

$$v_r = A/r, \tag{10}$$

where A is the constant subject to determination.

Having integrated (9), with consideration of (10), we obtain

$$p = p_0 + fA^2/r, \tag{11}$$

where p_0 is the integration constant.

With consideration of (5), (10), and (11), the total pressure difference across an ideal reactor will be equal to

$$\Delta p = A^2\left[\frac{\sigma_1}{R_1^2} + \frac{\sigma_2}{R_2^2} + f\left(\frac{1}{R_1} - \frac{1}{R_2}\right)\right]. \tag{12}$$

The velocity of the gas at the inlet zone I is determined from the condition of flow-rate constancy:

$$v_{\text{вх}}(2L/R_1)\,v_{r,1} = 2LA/R_1^2. \tag{13}$$

The pressure difference $\Delta p_c = \rho v_{in}^2/2$ along the distributing collector in dimensionless form, with consideration of (12) and (13), is written as follows:

$$\Delta\tilde{p}_c = \frac{\Delta p_c}{\Delta p} = \frac{2\rho L^2}{R_1^4}\left[\frac{\sigma_1}{R_1^2} + \frac{\sigma_2}{R_2^2} + f\left(\frac{1}{R_1} - \frac{1}{R_2}\right)\right]. \tag{14}$$

It is obvious that the distribution of the flow in a radial apparatus will be uniform when $\Delta\tilde{p}_c \ll 1$. With a reduction in the resistance of the system Δp and v_{in} are diminished (or the flow rate Q) in comparison with an ideal reactor. In this case, $\Delta\tilde{p}_c$ increases and the velocity profiles in zone III become nonuniform. Let us introduce the coefficient for the reduction in the flow rate as the characteristic for the magnitude of the flow nonuniformity:

$$\eta = (v_{in} - v_{in}^p)/v_{in} \tag{15}$$

and the degree of profile nonuniformity at the boundary Γ_1:

$$\xi = (v_{r,1}^{max} - v_{r,1}^{min})/\bar{v}_{r,1}, \tag{16}$$

where v_{in} is determined from formula (13), while v_{in}^p is determined numerically from the model.

In order to determine the relationship of η and ξ on $\Delta\tilde{p}_c$, we carried out calculations of the flows in various types of apparatus with different hydraulic characteristics and geometric dimensions. The initial data for the calculations are given in Table 1, while the results of the calculations can be found in Fig. 4a. It follows from this that the sought relationships fall within a range of variations in $\Delta\tilde{p}_c$ = 0-2.5, which is interesting from the standpoint of engineering application, and can be represented with good accuracy by the linear relationships

$$\eta = \Delta\tilde{p}_c/6; \quad \xi = \Delta\tilde{p}_c/2. \tag{17}$$

Relationships (17) are universal and weakly dependent on the geometric and hydraulic characteristics of the reactor over a rather broad range of variations in these quantities. With uniform permeability of the granular layer, the area of application for relationships (17) is limited only by the conditions of flow potential and the incompressibility of the fluid, which are satisfied in the majority of the types of apparatus used in actual practice.

Let us examine the examples of practical application for the proposed engineering methodology.

Let us calculate the optimum dimensions of an industrial ethyl-benzene dehydration reactor using a K-24 catalyst with a hydraulic drag coefficient of f = 8330 kg/m^4 and a contact gas flow rate of Q = 50 m^3/sec, where the density under operating conditions is ρ = 0.8 kg/m^3.

The maximum pressure drop across the reactor is Δp = 15,200 Pa (0.15 atm), and the maximum permissible stay time of the raw material in the distributing collector (zone I) is τ_I = 0.15 sec, the contact time of the vapor hydrocarbon mixture with the catalyst is τ_{III} = 1 sec, while the stay time of the contact gas in the outlet collector is τ_{II} = 0.25 sec.

Assuming that $[(\sigma_1/R_1^2) + (\sigma^2/R_2^2)] \ll f[(1/R_1) - (1/R_2)]$ and $R_1 \ll R_2$, with consideration of (10) and the fact that $Q = 2\pi R_1 L v_{r,1}$, from expression (12) we obtain

$$L^2R_1 \geqslant \frac{Q^2 f}{4\pi^2\Delta p}. \tag{18}$$

Since $\tau_I = V_I/Q = \pi R_1^2 L/Q$, we have

$$LR_1^2 \leqslant \tau_I Q/\pi. \tag{19}$$

The region A situated above the curve *a* satisfies inequality (18), while the region B below the curve b (Fig. 4b) satisfies inequality (19). The dimensions of the reactor which satisfy both of these conditions are found in region C within the intersection of A and B.

Under the assumptions made here, from expression (14) we have $\Delta\tilde{p}_c = 2\rho L^2/R_1^3 f$. Knowing that $\xi = \Delta\tilde{p}_c/2$, we obtain

$$L^2/R_1^3 = \xi f/\rho. \tag{20}$$

Figure 4b shows a family of curves (20) for various degrees of nonuniformity ξ. We see that if the reactor has dimensions of the region D bounded by the curves a, b, and 1, then the maximum nonuniformity in such an apparatus will be 20%. For $\xi = 0.1$ the region of permissible dimensional values becomes constricted, while in the case of $\xi = 0.01$ it is impossible to attain the optimum, since curve 4 does not intersect with region C. From Fig. 4b we can determine the optimum dimensions of the ethyl-benzene dehydration reactor in which we will have the minimum possible degree of nonuniformity $\xi = 0.05$: $L = 8.2$ m, $R_1 = 0.53$ m.

The diameter of the outlet collector is determined on the basis of the average contact time between the reaction mixture and the catalyst. It is obvious that $\tau_{III} = V_{III}/Q = \pi(R_2^2 - R_1^2)L/Q$, from which we find $R_2 = \sqrt{\tau_{III}Q/(\pi L) + R_1^2} = 1.5$ m.

The stay time in the outer collector can be estimated approximately as $\tau_{II} = V_{II}/Q = \pi(R_{ap}^2 - R_2^2)L/Q$, so that $R_{ap} = \sqrt{\tau_{II}Q/(\pi L) + R_2^2} = 1.65$ m.

Thus, as a result of simple calculations we can determine the dimensions of the ethylbenzene dehydration reactor with a given pressure difference, contact-gas stay times in the collectors, and the catalyst layer in which the minimum possible degree of nonuniformity occurs.

As is well known [7], the nonuniformities may significantly reduce the process indices (conversion, output yield), occurring within the catalyst layer, which is generally not taken into consideration in the design calculations. Preliminary estimates of the magnitude of the flow nonuniformity allows us to determine the true values of the process indices, even in cases in which it becomes necessary to alter the design of the apparatus.

Particular stress should be placed on the applicability of function (17) to the design of various types of equipment used extensively in actual practice. Thus, when $\sigma_1 \neq 0$, $f = 0$, $\sigma_2 = 0$ we have a perforated distributing collector that is used in ventilation systems; when $\sigma_1 = 0$, $f \neq 0$, together with an arbitrary σ_2, or when $\sigma_1 = \sigma_2 = 0$, $f \neq 0$, we have the model of a chemical reactor with a radial granular or block-catalyst layer, or a filtration installation; when $\sigma_1 \neq 0$, $f \neq 0$, $\sigma_2 = 0$ and $R_2 \to \infty$, we have a system that is used in subsoil irrigation for purposes of land reclamation.

NOTATION

r, z, the coordinate axes; $\mathbf{v}$, the velocity vector; v, the velocity component; $\tilde{v}$, normalized value of the velocity component; $\bar{v}$, average value of the velocity component; u, the velocity amplitude; p, pressure; Δp, the pressure difference across the apparatus; Δp_c, the pressure difference across the distributing collector; R_1, the radius of the distributing collector; R_2, the radius of the outlet collector; R_{ap}, the radius of the apparatus; L, the height of the apparatus; V, the volume; Q, the flow rate; τ, the stay time; $f = 1.75\rho(1 - \varepsilon)/d\varepsilon^3$, the coefficient of granular-material resistance; ε, the porosity of the granular medium; ρ, the density of the liquid or the gas; d, the effective grain diameter; $\sigma_{1,2}$, represents the coefficients of collector drag; η, the coefficient of flow-rate reduction; ξ, the degree of flow nonuniformity. Subscripts: r identifies the radial components; z denotes the axial component; 1, 2 represent the boundaries Γ_1 and Γ_2; in denotes the inlet to the distributing collector; out identifies the outlet from the apparatus; I, II, and III identify the zones I, II, III.

LITERATURE CITED

1. V. S. Genkin, V. V. Dil'man, and S. P. Sergeev, Gazovoe Delo, No. 7, 10-13 (1972).
2. A. S. Nazarov, V. V. Dil'man, and S. P. Sergeev, Inzh.-Fiz. Zh., 41, No. 5, 1009-1015 (1981).
3. I. V. Shirko, R. V. Sarkisov, D. N. Motyl', and V. V. Dil'man, Teor. Osn. Khim. Tekhnol., 20, No. 2, 211-217 (1986).
4. P. G. Shtern, E. A. Rudenchik, S. V. Turuntaev, and G. N. Abaev, The Aerodynamics of Chemical Reactors with Nonmoving Catalyst Layers [in Russian], Novosibirsk (1985), pp. 67-80.
5. S. Ergun, Chem. Eng. Progr., 48, 88-93 (1952).

6. I. E. Idel'chik, Handbook on Hydraulic Drag [in Russian], Moscow (1975).
7. I. S. Luk'yanenko, G. N. Abaev, and E. K. Popov, The 1st All-Union Symposium on Macroscopic Kinetics and Chemical Gasdynamics, Chernogolovka (1984), Vol. 2, Ch. 1, p. 44.

THE COMPLETE FILLING OF DEAD-END CONICAL CAPILLARIES WITH LIQUID

G. I. Dovgyallo, N. P. Migun, and P. P. Prokhorenko

UDC 532.6

We have observed the complete bilateral filling of dead-end conical capillaries with liquid, which is accompanied by the rapid dissolving of the air enclosed within the cavities.

We know that the nature of filling a dead-end capillary depends to a significant degree on the extent to which the gas enclosed within its cavity is dissolved and diffused into the liquid [1]. If the gas is poorly dissolved in the liquid, then in capillaries of a length $\ell_0 < 10^{-3}$ m and radius $R > 0.5$ μm during the time $t < 1$ sec a limit filling depth ℓ_∞ is established, which is defined by the equality of the capillary pressure and the pressure of the compressed air. As was demonstrated in [2], for conical capillaries the theoretical and experimental values of ℓ_∞ are in good agreement. In the case of good solubility and diffusion of the air in the liquid filling the capillaries, the depth of this filling may be considerably greater than ℓ_∞. A study was undertaken in [3] for the case in which dead-end conical capillaries are filled with defectoscopic liquids, when the meniscus continues rather rapidly to shift into the depth of the channel after establishment of the limit depth ℓ_∞.

Below we describe the results from the study into the filling of dead-end small-dimension capillaries (with a length of 30 μm $< \ell_0 < 10^3$ μm and a radius 0.4 μm $< R <$ 15 μm) with various liquids, thus making it possible to establish that in a number of cases the capillary is filled not only from the inlet side of the channel, but from the top as well. In this case, at the instant that the capillary is completely filled, the volume of liquid formed at the top and moving toward the inlet may be greater than half the total volume of liquid within the capillary.

We used dead-end conical and cylindrical capillaries which had been drawn, by means of a burner, out of cylindrical glass tubing, immediately prior to the experiment. The capillary was glued horizontally to the bottom of the vessel which was being filled with the liquid. A "Biolam-R-16" microscope was used to observe the displacement of the menisci of the liquid in the capillary. The measurement error amounted to ±0.5 μm.

The capillaries were filled with distilled water, ethyl alcohol, acetone, and kerosene. For the first of the three liquids, in each of the conical capillaries we observed the formation and subsequent growth in a cone of liquid at the apex of the channel (Fig. 1). Figure 2 illustrates the kinetics of the growth in each of the liquid volumes in the capillary. Within a specified period of time (4.4 h in Fig. 2) both fluid columns combine and the capillary is completely filled. As the dimensions of the capillary are reduced, the time required for the complete filling of the capillary is also shortened. For example, 415 sec are needed to fill completely a conical capillary with dimensions $\ell_9 = 210$ μm and $R = 4$ μm with distilled water. The conical capillaries were filled considerably more quickly with kerosene than with water, and this was not accompanied by any noticeable growth in the small column at the apex of the capillary, formed as a consequence of capillary condensation (the volume of this column amounted to $V_C < 10^{-3}V_0$, where V_0 is the total volume of the capillary channel).

Institute of Applied Physics, Academy of Sciences of the Belorussian SSR, Minsk. Translated from Inzhenerno-Fizicheskii Zhurnal, Vol. 56, No. 4, pp. 563-565, April, 1989. Original article submitted November 5, 1988.